Clin Neuroradiol (2019) 29:45–50
https://doi.org/10.1007/s00062-017-0626-4

ORIGINAL ARTICLE

Proton Density Fat Suppressed MRI in 3T Increases the Sensitivity of Multiple Sclerosis Lesion Detection in the Cervical Spinal Cord

Efstratios Karavasilis[1] · George Velonakis[1] · George Argiropoulos[1] · Athanasios Athanasakos[1] · Loukia S Poulou[1] · Panagiotis Toulas[1] · Nikolaos L Kelekis[1] · Efstathios P Efstathopoulos[1]

Received: 11 July 2017 / Accepted: 2 September 2017 / Published online: 26 September 2017

Abstract
Purpose Considering the number of multiple sclerosis (MS) patients referred for clinical spinal cord imaging, the optimization of imaging protocols plays a crucial role. We aimed to evaluate the use of proton density (PD) turbo spin-echo (TSE) with spectral attenuated inversion recovery (SPAIR) fat suppression and compare it with the currently recommended T2-TSE-SPAIR in sagittal plane in cervical spinal cord imaging.
Methods In this study 35 MS patients with clinically suspected or known spinal cord lesions were scanned on a 3.0T magnetic resonance imaging (MRI) system. In addition to the routine protocol, PD-TSE-SPAIR sequences were obtained to quantitatively and qualitatively evaluate lesion detectability and image quality compared to T2-TSE-SPAIR sequences. Quantitative analysis was based on measurements of lesion-to-cord contrast ratio (LCCR), lesion contrast-to-noise ratio (LCNR) and lesion dimensions and the qualitative analysis on ranking with a predetermined score scale. The presence of lesions in these sequences was verified in axial T2 multi-echo gradient echo images.
Results In quantitative analysis, the lesions on PD-TSE-SPAIR had statistically significantly higher contrast ($p < 0.05$), according to the statistical test of LCCR, LCNR calculated contrast and measured lesion dimensions. Qualitative analyses were congruent with quantitative results; the median rank of PD-TSE-SPAIR was significantly higher than T2-TSE-SPAIR ($p < 0.05$). Of the 34 detected lesions 9 (26%) were not visualized in T2-TSE-SPAIR sequence.
Conclusion Considering its superiority in contrast ratios and lesion dimensions when compared to T2-TSE-SPAIR in both qualitative and quantitative analyses, we therefore recommend PD-TSE-SPAIR as a pivotal sequence to evaluate demyelinating spinal cord lesions at 3T.

Keywords Multiple sclerosis · Cervical spinal cord · Magnetic resonance

Introduction

Multiple sclerosis (MS) is a chronic inflammatory disease that involves an attack on central nervous system (CNS). The disease corresponds to damaged myelin, which leads to the formation of scar tissue or sclerosis [1, 2]. Since 2001, magnetic resonance imaging (MRI) has been incorporated into the overall diagnostic scheme as proposed by the McDonald International Panel criteria, which also became the gold standard for MS diagnosis [3, 4]. The current revised McDonald criteria increased sensitivity from 60% to 72% compared to 2005 without optimizing specificity, which was 87% compared to 88% in 2005 [5].

The published guidelines of the Consortium of MS Centers aim to standardize brain and spinal cord MRI protocols [6, 7]. The most recently revised guidelines for spinal cord include sagittal T1 and proton density-weighted, T2-weighted combined with short tau inversion recovery (STIR) or spectral presaturation with inversion recovery (SPIR) fat suppression, axial T2 or T2*-weighted imaging for suspicious lesions and post-contrast gadolinium-enhanced T1-weighted imaging in some cases [8]. Thus, considering the number of MS patients referred for clinical

✉ Efstratios Karavasilis
stratoskaravasilis@yahoo.gr

[1] Second Department of Radiology, University General Hospital 'Attikon', School of Medicine, National and Kapodistrian University of Athens, Athens, Greece

spinal cord imaging in routine radiological practice, we aimed to evaluate the use of proton density (PD) with spectral attenuated inversion recovery (SPAIR) fat suppression and compare it with the currently recommended T2 fat suppression in the sagittal plane.

Material and Methods

All participants gave their informed consent to participate in this study, which was conducted according to the Declaration of Helsinki and was approved by the institutional local ethical committee.

Subjects

A total of 35 patients who presented for assessment in our institute between February 2016 and May 2016 with diagnosed MS, and clinically suspected or confirmed spinal cord lesions were consecutively included in our study. Examinations with the presence of either motion artifacts due to non-compliant subjects or with ghosting artifacts were excluded from our sample.

Magnetic Resonance Imaging Protocol

Imaging data were acquired on a 3T Philips MRI scanner (Achieva TX, Philips, Healthcare, Best, the Netherlands) equipped with a 16-channel sensitivity-encoding head and neck coil. The imaging protocol included:

1. sagittal T2-weighted turbo spin-echo (TSE),
2. sagittal T2-weighted TSE combined with SPAIR technique for fat suppression,
3. sagittal T1-weighted TSE,
4. sagittal PD weighted TSE-SPAIR,
5. axial T2-weighted multi echo fast field echo (mFFE) and
6. axial T1-weighted TSE.

The T1-weighted sequences were repeated after gadolinium injection with the exception of patients who had previously had cervical spine MRI. In these cases precontrast T1-weighted images were not acquired. Detailed imaging parameters of the sequences used are listed in Table 1.

Image quality control was assessed reviewing all images by an MRI physicist in collaboration with one of the two experienced neuroradiologists. Of the scans five were excluded due to the presence of artifacts, three due to the presence of motion artifacts and two due to ghosting artifacts in both T2-TSE-SPAIR and PD-TSE-SPAIR sequences. Neuroradiologists reviewed all the images confirming the presence of a demyelinating plaque visualized at least in two sequences. Lesions visualized only in one sequence were re-evaluated to assess whether it could be retrospectively identified in other sequences. Our study had two parts, the quantitative and qualitative analysis of T2-TSE-SPAIR and PD-TSE-SPAIR sequences.

Magnetic Resonance Imaging Analysis

Quantitative Analysis

Quantitative measurements of the lesions were obtained using an EVORAD workstation. To maximize the visibility of spinal cord lesion we adjusted variation of window widths and levels. To determine lesion-to-cord contrast ratio (LCCR) and lesion contrast-to-noise (LCNR) we drew three regions of interest (ROIs), as previously described in the literature [9]:

a) within the spinal lesions (S_{lesion}) on the sequence in which they were most readily identified,
b) in the normal appearing cervical cord (S_{cord}) avoiding regions of artifacts and
c) to the air background near to the tissue.

These ROIs were superimposed on the remaining sequence using the copy-paste feature of EVORAD (Evorad SA, Athens, Greece, www.evorad.com). Sets of values

Table 1 Detailed imaging parameters of the used sequences

Sequence	TR (ms)	TE (ms)	Inversion delay (ms)	ST (mm)	Slices (*n*)	Matrix (pixels)	FOV (cm × cm)	Acquisition time
T2-TSE-SPAIR	3000	80	140	3	15	512 × 512	22.3 × 22.3	4 min 18 s
PD-TSE-SPAIR	3000	30	140	3	15	512 × 512	22.3 × 22.3	4 min 18 s
T2-TSE	3040	75	–	3	15	528 × 528	23.3 × 23.3	2 min 19 s
T1-TSE	429	8	–	3	15	480 × 480	23.3 × 23.3	2 min 31 s
AxT2-mFFE	7000	6.44/14.44/22.44/30.44/38.44	–	3	27	672 × 672	20.0 × 20.0	4 min 58 s
AxT1-TSE	667	7.86	–	3	27	512 × 512	24.0 × 24.0	4 min 18 s

ST slice thickness, *SPAIR* spectral attenuated inversion recovery, *PD* proton density, *AxT2* axial T2-weighted, *AxT1* axial T1-weighted, *mFFE* multi echo fast field echo, *ms* millisecond, *cm* centimeters, *FOV* field of view, *TSE* turbo spin echo

were obtained for all lesions in the acquired two sequences. The LCCR and LCNR were calculated for each sequence by the measurements of the above ROIs using the equations 1 and 2, respectively.

$$LCCR = \frac{(S_{lesion} - S_{cord})}{S_{cord}} \quad (1)$$

$$LCNR = \frac{(S_{lesion} - S_{cord})}{SD_{air}} \quad (2)$$

SD_{air} = standard deviation of the pixel signal intensities within the drawn ROI on the background

Additionally, the craniocaudal extension (CCE) and the axial (anteroposterior) diameter (AD) of the lesions were measured in both sequences as a criterion of the sensitivity on lesion size, adjusting the optimal image contrast to better clarify lesion edges.

Qualitative Analysis

In this study two experienced radiologists (raters), blinded to the pathology of patient data, reviewed all images to detect the cord lesions on calibrated, high-resolution monitors provided by the institutional medical workstation, 1 month after scanning. Qualitative analysis was completed in two stages (stage I and stage II). At the first (stage I), raters detected and recorded the number and the location of the lesions separately in each T2-TSE-SPAIR and PD-TSE-SPAIR sequence, identified in sagittal T2-TSE and axial-T2- mFFE sequences. Then, the individual set of images was independently viewed side-by-side to rank the sensitivity of lesion detection using a predetermined 4-point rating scale (stage II). Raters used the rating scale based on the following assumptions: score 4 images where lesions had high contrast (i. e. the lesion edges were well discriminated), score 3 images where all lesions were detected but with lower contrast (i. e. the lesion edges were not easily visible), score 2 images with at least one missed lesion and score 1 images with at least two missed lesions.

Statistical Analysis

Nonparametric Wilcoxon test was used to compare the calculated quantitative ratios, the dimensions and the observers' score between the two sequences. All analyses were conducted using the IBM Statistical Package for Social Sciences (SPSS) version 22.0 and the level of statistical significance was set at $p < 0.05$.

Results

The mean age of the included patients was 39.88 ± 11.03 years, and the female/male ratio was 17:9. In 26 out of the 35 patients (74%), 34 MS lesions were identified within the cervical spinal cord.

Quantitative Measures

The lesions on PD-TSE-SPAIR had statistically significantly higher contrast ($p < 0.05$), estimated from non-

Table 2 Nonparametric statistical tests of the comparison of PD-TSE-SPAIR and T2-TSE-SPAIR sequences, using LCCR and LCNR contrast ratios

Sequence/Contrast	Descriptive statistics			Percentiles			Statistics (p-value)
	N	Mean	SD	25th	50th (median)	75th	
PD-TSE-SPAIR/LCNR	34	27.14	15.14	16.70	22.36	32.97	>0.05
T2-TSE-SPAIR/LCNR	34	12.91	16.07	4.02	7.14	14.24	
PD-TSE-SPAIR/LCCR	34	0.30	0.14	0.20	0.28	0.36	>0.05
T2-TSE-SPAIR/LCCR	34	0.20	0.21	0.09	0.11	0.28	

SPAIR spectral attenuated inversion recovery, *PD* proton density, *LCCR* lesion-to-cord contrast ratio, *LCNR* lesion contrast-to-noise, *SD* standard deviation

Table 3 Nonparametric statistical tests on the comparison of PD-TSE-SPAIR and T2-TSE-SPAIR sequences, using CCE and AD lesion dimensions

Sequence/contrast	Descriptive statistics			Percentiles			Statistics (p-value)
	N	Mean	SD	25th	50th(median)	75th	
PD-TSE-SPAIR/AD	34	0.40	0.12	0.31	0.39	0.48	>0.05
T2-TSE-SPAIR/AD	34	0.25	0.18	0.00	0.29	0.39	
PD-TSE-SPAIR/CCE	34	1.29	0.81	0.70	1.00	1.50	>0.05
T2-TSE-SPAIR/CCE	34	0.66	0.64	0.00	0.57	0.86	

AD axial dimension, *CCE* craniocaudal extension, *SD* standard deviation, *SPAIR* spectral attenuated inversion recovery, *PD* proton density, *TSE* turbo spin-echo

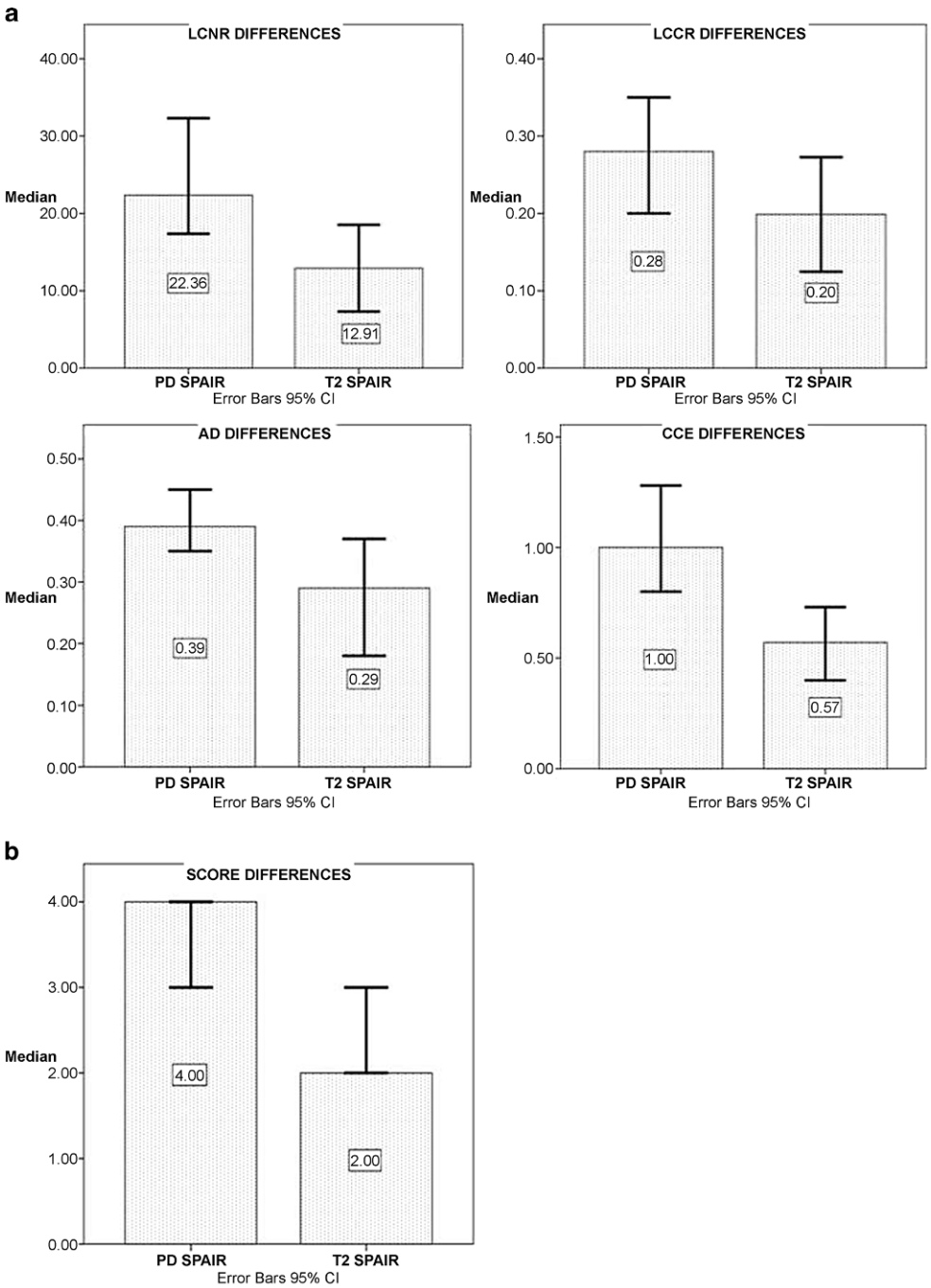

Fig. 1 Nonparametric statistical tests of the comparison of PD-TSE-SPAIR and T2-TSE-SPAIR sequences using (**a**) quantitative measures (for LCCR and LCNR contrast ratios, CCE and AD lesion dimensions) and (**b**) qualitative measures (predetermined rating scale of visual inspection of two independent raters) (*LCCR* lesion-to-cord contrast ratio, *LCNR* lesion contrast-to-noise ratio, *AD* axial diameter, *CCE* craniocaudal extension, *SPAIR* spectral attenuated inversion recovery, *PD* proton density)

parametric Wilcoxon statistical test of LCCR and LCNR calculated contrasts, as shown in the box plots (Fig. 1).

The LCCR and LCNR median values of 34 detected lesions were 2.4 and 3.1 times higher on PD-TSE-SPAIR, respectively, with the first and third quartile deviations keeping the difference statistically high (Table 2).

The PD-TSE-SPAIR sequence showed a significantly higher sensitivity on lesion size compared with T2-TSE-SPAIR sequences (Fig. 1). Both CCE and AD lesion dimensions differed significantly ($p < 0.05$) (Table 3).

Qualitative Measures

The results of qualitative analyses were congruent with quantitative results; all lesions on the PD-TSE-SPAIR, in contrast to T2-TSE-SPAIR, were statistically significantly different from background spinal cord and were also all readily visible. The median rank of PD-TSE-SPAIR was significantly higher than T2-TSE-SPAIR ($p < 0.05$), as shown in box plot diagram (Fig. 1). Of the 34 detected

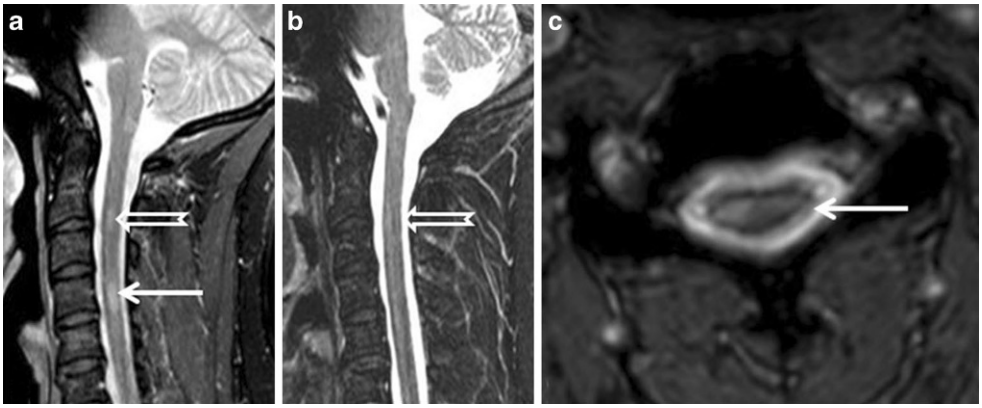

Fig. 2 **a** PD-TSE-SPAIR sagittal, **b** T2-TSE-SPAIR sagittal, **c** T2-mFFE axial images. The lesion at C2-C3 level is better visualized on PD-SPAIR (*empty arrow*, **a**) compared with T2-TSE-SPAIR (*empty arrow*, **b**). The lesion visualized at C4 level on PD-TSE-SPAIR (*solid arrow*, **a**) verified on axial T2-mFFE (*solid arrow*, **c**), is not visible on T2-TSE-SPAIR (**b**) (*SPAIR* spectral attenuated inversion recovery, *PD* proton density, *mFFE* multi echo fast field echo)

lesions 9 (26%) were not visualized in T2-TSE-SPAIR sequence (Fig. 2).

Discussion

This article highlights the advantage of PD-SPAIR in detecting both the number and the size of MS spinal cord lesions compared to T2-TSE-SPAIR sequence. Specifically, the PD-TSE-SPAIR technique identified significantly more lesions combined with improved quality in qualitative assessment, and statistically significantly higher contrast ratios (LCCR, LCNR) and lesion size measurements in quantitative assessment. The changes in longitudinal dimension of lesions demonstrate the capability of PD-TSE-SPAIR imaging to depict long lesions, which appeared as multiple small lesions in T2-TSE-SPAIR.

Spinal cord MRI can establish an early diagnosis in MS and recognize clinical subtypes of MS. Due to this advantage, there are an increasing number of research projects trying to improve lesion detectability by comparing different techniques of imaging [9–15]. According to guidelines, PD imaging is proposed to be included in the core imaging protocol of MS cervical cord imaging [6–8]. Moreover, MRI findings of PD imaging showed significant correlation with histopathological results of MS plaques [16]. A recent study demonstrated the diagnostic benefit of PD-TSE imaging comparing to T2-TSE imaging using a large cohort of MS patients. Chong et al. found statistically significant differences in CNR (PD:82 vs T2:64) between the two imaging contrasts, with 19% more detectable lesions in PD imaging [9]. The T2-weighted to short tau inversion recovery (STIR) comparisons show high sensitivity to detect demyelinating lesions [10–12]. The increase of sensitivity was quantified as up to 10% more detected lesions [13]. Fluid attenuation inversion recovery (FLAIR) sequences lack sufficient sensitivity and specificity in spinal cord imaging because it is influenced by cerebrospinal fluid (CSF) pulsation artifacts in spite of its superiority at brain lesion detectability. The FLAIR has the lowest CNR set against T2-weighted and SPIR results (13.87 vs. 7.43 vs. 4.69) [12]. Based on these published results, we assumed that adding pre-pulse in PD-TSE sequence to suppress the signal of fat we would improve the image contrast. The image contrast is defined by the signal of the neighboring tissues and by suppressing fat signals, all the tissues, such as bones, fluids and cord lesions are brightened, thus the total contrast of the image is increased.

The strength of our study includes the application of two comparative approaches (i. e. qualitative and quantitative analyses) with their results being in agreement. Apart from the relatively small sample size, the major limitation of our study is the absence of T2-STIR weighted images, which would be compared with T2 and PD-TSE-SPAIR images; however, the T2-TSE-SPAIR sequence is relatively independent of the T1 longitudinal relaxation time compared to T2-STIR sequences [17]. The T1 relaxation time of some tissues is shortened due to the paramagnetic contrast agent, which increases the possibility of signal suppression of non-fatty tissues [18]. To increase the sensitivity of active MS lesion detection in post-gadolinium T1 images due to T1-weighted late enhancement imaging [19] it is our institutional practice to inject gadolinium contrast agent immediately after T1 sequences following by T2 and PD-weighted sequences. Considering the abovementioned STIR disadvantages and lower signal-to-noise ratio compared to T2-TSE-SPAIR due to non-selective inversion 180^0 pulse, we did not include T2-STIR sequences in our imaging protocol.

Conclusion

Considering its superiority in contrast ratios and lesion dimensions when compared to T2-TSE-SPAIR in both qualitative and quantitative analyses, we highlight PD-TSE-SPAIR as a pivotal sequence to evaluate demyelinating spinal cord lesions at 3T. Future studies could further evaluate PD-TSE-SPAIR, which could be introduced in the core MS spinal cord imaging protocol as a potential alternative to T2-TSE-SPAIR.

Acknowledgements We thank all participants for their willingness to participate in the present study.

Compliance with ethical guidelines

Conflict of interests E. Karavasilis, G. Velonakis, G. Argiropoulos, A. Athanasakos, L.S. Poulou, P. Toulas, N.L. Kelekis and E.P. Efstathopoulos declare that they have no competing interests.

Ethical standards All procedures performed in studies involving human participants were in accordance with the ethical standards of the institutional and/or national research committee and with the 1964 Helsinki declaration and its later amendments or comparable ethical standards. Informed consent was obtained from all individual participants included in the study.

References

1. Grigoriadis N, van Pesch V; ParadigMS Group. A basic overview of multiple sclerosis immunopathology. Eur J Neurol. 2015;22 Suppl 2:3-13.
2. Noseworthy JH, Lucchinetti C, Rodriguez M, Weinshenker BG. Multiple sclerosis. N Engl J Med. 2000;343(13):938–52.
3. McDonald WI, Compston A, Edan G, Goodkin D, Hartung HP, Lublin FD, McFarland HF, Paty DW, Polman CH, Reingold SC, Sandberg-Wollheim M, Sibley W, Thompson A, van den Noort S, Weinshenker BY, Wolinsky JS. Recommended diagnostic criteria for multiple sclerosis: guidelines from the international panel on the diagnosis of multiple sclerosis. Ann Neurol. 2001;50(1):121–7.
4. Ntranos A, Lublin F. Diagnostic criteria, classification and treatment goals in multiple sclerosis: the chronicles of time and space. Curr Neurol Neurosci Rep. 2016;16(10):90.
5. Swanton JK, Rovira A, Tintore M, Altmann DR, Barkhof F, Filippi M, Huerga E, Miszkiel KA, Plant GT, Polman C, Rovaris M, Thompson AJ, Montalban X, Miller DH. MRI criteria for multiple sclerosis in patients presenting with clinically isolated syndromes: a multicentre retrospective study. Lancet Neurol. 2007;6(8):677–86.
6. Traboulsee A, Li D, Frank J, Simon J, Coyle P, Wolinsky J, Paty D. Consortium of MS Centers. MRI Protocol for the Diagnosis and Follow-up of MS. 2003. http://www.mscare.org/resource/collection/9C5F19B9-3489-48B0-A54B-623A1ECEE07B/MRIprotocol2003.pdf
7. Consortium of MS Centers. MRI Protocol for the Diagnosis and Follow-up of MS. 2009 Revised Guidelines. http://www.mscare.org/resource/collection/9c5f19b9-3489-48b0-a54b-623a1ecee07b/mriprotocol2009.pdf?hhSearchTerms=%22MRIprotocol2009%22
8. Traboulsee A, Simon JH, Stone L, Fisher E, Jones DE, Malhotra A, Newsome SD, Oh J, Reich DS, Richert N, Rammohan K, Khan O, Radue EW, Ford C, Halper J, Li D. Revised recommendations of the consortium of MS centers task force for a standardized MRI protocol and clinical guidelines for the diagnosis and follow-up of multiple sclerosis. AJNR Am J Neuroradiol. 2016;37(3):394–401.
9. Chong AL, Chandra RV, Chuah KC, Roberts EL, Stuckey SL. Proton density MRI increases detection of cervical spinal cord multiple sclerosis lesions compared with T2-weighted fast spin-echo. AJNR Am J Neuroradiol. 2016;37(1):180–4.
10. Rocca AM, Mastronardo G, Horsfield AM, Pereira C, Iannucci G, Colombo B, Moiola L, Comi G, Filippi M. Comparison of three MR sequences for the detection of cervical cord lesions in patients with multiple sclerosis. AJNR Am J Neuroradiol. 1999;20(9):1710–6.
11. Campi A, Pontesilli S, Gerevini S, Scotti G. Comparison of MRI pulse sequences for investigation of lesions of the cervical spinal cord. Neuroradiology. 2000;42(9):669–75.
12. Hittmair K, Mallek R, Prayer D, Schindler EG, Kollegger H. Spinal cord lesions in patients with multiple sclerosis: comparison of MR pulse sequences. AJNR Am J Neuroradiol. 1996;17(8):1555–65.
13. Philpott C, Brotchie P. Comparison of MRI sequences for evaluation of multiple sclerosis of the cervical spinal cord at 3T. Eur J Radiol. 2011;80(3):780–5.
14. Gerigk L, Bostel T, Hegewald A, Thomé C, Scharf J, Groden C, Neumaier-Probst E. Dynamic magnetic resonance imaging of the cervical spine with high-resolution 3-dimensional T2-imaging. Clin Neuroradiol. 2012;22(1):93–9.
15. Wattjes MP, Steenwijk MD, Stangel M. MRI in the diagnosis and monitoring of multiple sclerosis: an update. Clin Neuroradiol. 2015;25(S2):157–65.
16. Nijeholt GJ, Bergers E, Kamphorst W, Bot J, Nicolay K, Castelijns JA, van Waesberghe JH, Ravid R, Polman CH, Barkhof F. Post-mortem high-resolution MRI of the spinal cord in multiple sclerosis: a correlative study with conventional MRI, histopathology and clinical phenotype. Brain. 2001;124(1):154–66.
17. Uysal E, Erturk SM, Yildirim H, Seleker F, Basak M. Sensitivity of immediate and delayed gadolinium-enhanced MRI after injection of 0.5M and 1.0M gadolinium chelates for detecting multiple sclerosis lesions. AJR Am J Roentgenol. 2007;188(3):697–702.
18. Krinsky G, Rofsky NM, Weinreb JC. Nonspecificity of short inversion time inversion recovery (STIR) as a technique of fat suppression: pitfalls in image interpretation. AJR Am J Roentgenol. 1996;166(3):523–6.
19. Kaldoudi E, Williams SC, Barker GJ, Tofts PS. A chemical shift selective inversion recovery sequence for fat-suppressed MRI: theory and experimental validation. Magn Reson Imaging. 1993;11(3):341–55.